euspen's 25th International Conference & Exhibition, Zaragoza, ES, June 2025
www.euspen.eu

Effect of mist spray conditions on machining characteristics in direct engraving milling of high-hardness mould material

Takeru Minamide[1], Hideharu Kato[2], Shigehiko Sakamoto[2], Masahiro Furuno[3]

[1]*Graduate School of Engineering, Kanazawa Institute of Technology, Japan*
[2]*Department of Mechanical Engineering, Kanazawa Institute of Technology, Japan*
[3]*Professional Engineer, MOLDINO The Edge To Innovation, Japan*

c6400491@st.kanazawa-it.ac.jp

Abstract

Plastic moulds for moulding in corrosive gas environments are often made of martensitic stainless steel (STAVAX) due to its excellent corrosion resistance. In mould manufacturing, machining processes such as heat treatment are used after preprocessing to form the shape of the raw material by cutting. Direct engraving milling can shorten the machining process. However, because STAVAX has high adhesion, direct engraving milling often leads to tool damage and adhesion to the machined surface, reducing surface precision. A previous study conducted direct engraving milling under high-cutting-speed conditions in a minimum quantity lubrication environment and found that wear of the end cutting edge, which forms the machined surface, and adhesion to the machined surface were suppressed, enabling high-efficiency machining. However, significant damage occurred on the side cutting edge that removes the workpiece, leading to poor tool life. In this study, the effect of mist spray conditions on machining characteristics was investigated by cutting inclined surfaces of STAVAX with a small-diameter-ball end mill using a downward pick feed, assuming side cutting of a mould. It was found that increasing the mist flow velocity effectively suppressed flank wear progression on the side cutting edge. Mist velocity did not affect the flank wear of the end cutting edge. A surface analysis showed that all mist conditions achieved a surface roughness Rz of 0.07 µm or lower.

STAVAX, small-diameter ball end mill, mist, direct engraving milling

1. Introduction

Plastic moulds for moulding in corrosive gas environments are often made of martensitic stainless steel (STAVAX) due to its excellent corrosion resistance [1-2]. The mould manufacturing process, the raw material is first shaped by cutting, followed by heat treatment. Grinding is then carried out to remove any strain caused by the heat treatment, and finally, the surface is polished to a mirror finish [3]. These numerous steps result in longer machining times and increased costs [4]. For small moulds, direct engraving milling can shorten cutting time and reduce the number of required processes [5]. However, because STAVAX has high adhesion, direct engraving milling often leads to tool damage and adhesion to the machined surface, reducing surface precision and increasing postprocessing time [6]. In a previous study, direct engraving milling was attempted under high-cutting-speed conditions in a minimum quantity lubrication environment [7]. It was found that wear of the end cutting edge, which forms the machined surface, and adhesion to the machined surface were suppressed, enabling high-efficiency machining. However, significant damage occurred on the side cutting edge that removes the workpiece, leading to poor tool life. To improve efficiency, it is necessary to reduce damage to the side cutting edge. In this study, the effect of mist spray conditions on machining characteristics was investigated by performing direct engraving milling on STAVAX using a small-diameter-ball end mill.

2. Experimental procedure

The work material used was stainless steel (STAVAX) heat-treated to a hardness of HRC 52. A small-diameter-ball end mill was used. The balls had a diameter of 2.0 mm and were made of ultrafine-particle cemented carbide with a TiSiN coating. The experiment involved machining a 45° slope, as shown in Figure 1, using a downward pick feed to simulate the side cutting of a mould. The cutting conditions were as follows: a cutting speed (V) of 240 m/min, a cut depth (Ad) of 0.015 mm, a feed per tooth (fz) of 0.02 mm/tooth, and a pick feed (Pf) of 0.02 mm. Down-cut machining was used. A cutting environment that employed minimum quantity lubrication with three types of mist (Type A, Type B, and Type C) was used to investigate the effect of mist supply conditions. The type of mist requires different equipment to be used. Accordingly, the supply pressure, oil quantity, and flow rate vary. Table 1 shows the specifications and measurements of each type of mist. The flow velocity was measured at the centre of the mist spray using a Pitot tube, with the feed distance (DN) set to 40 mm. Although flow velocity could be adjusted by changing the supplied air pressure for Type B and Type C, standard values were used in this study. The flow rate was measured at the nozzle outlet. Tool wear conditions were measured using scanning electron microscopy (SEM; JSM-6390A, JEOL Ltd.). The mist spraying state and the mist supply state during machining were recorded using a high-speed camera (VW-9000, Keyence Corporation). The video was analysed using video editing and analysis software (VW-H2MA, Keyence Corporation). Figure 2 shows high-speed camera images of the spray conditions for each mist type. The measured

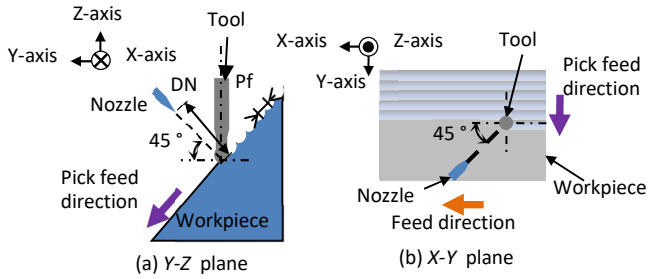

Figure 1. Schematic diagram of experimental setup

Table 1 Minimum quantity lubrication specifications and measurements

Type of oil			Type A	Type B	Type C
Density	ρ	[g/cm³]	0.96	0.89	0.93
Kinematic viscosity	v	[mm²/s]	35	13	8.9
Flow velocity	u	[m/s]	66.7	126	73.8
Flow rate	Q	[ml/h]	8.54	3.59	1.00

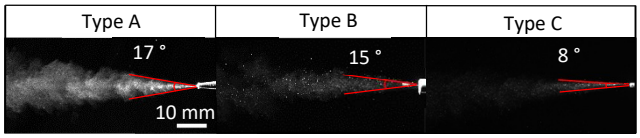

Figure 2. Comparison of minimum quantity lubrication spraying for three mist types

spray angles were 17° for Type A, 15° for Type B, and 8° for Type C. Type A and Type B had similar spray angles. Tool wear was observed at the side cutting edge, which removes material, and the end cutting edge, which contributes to forming the machined surface. Tool life was defined as the point where one of the following conditions was met: the flank wear width of the end cutting edge reached 20 µm, excessive flaking or failure occurred at the side cutting edge, or the maximum height roughness (Rz) exceeded 1 µm. Additionally, the cutting distance was defined not as the machined surface length but as the sliding distance of the cutting edge in actual contact.

3. Experimental results and discussion

3.1 Effect of mist spray conditions on machining characteristics

Figure 3 shows the flank wear rate of the side and end cutting edges for each mist condition. For the side cutting edge, Type B led to the slowest wear rate, followed by Type A and Type C in increasing order of wear. Figure 4 shows the wear condition of the side cutting edge at a cutting distance of 990 m. For Type B, the flank wear on the side cutting edge progressed gradually. In contrast, for Type A and Type C, coating flaking occurred at the lower part of the side cutting edge flank. To investigate the cause of this phenomenon, the characteristics and spray conditions of each mist type, as described in the experimental method, along with the supply conditions captured by the high-speed camera, were analysed. Figure 5 shows the mist supply conditions captured by the high-speed camera. As shown, Type B supplied lubricant to the side cutting edge flank, whereas Type A and Type C did not supply lubricant, and machining was performed with material resembling chips adhered to the cutting edge. Type B's high flow velocity allowed the oil to reach the machining point without being disrupted by the airflow caused by tool rotation, resulting in gradual wear without flaking. Although Type A had a large flow rate and spray angle, its low mist velocity led to inadequate mist supply to the machining point,

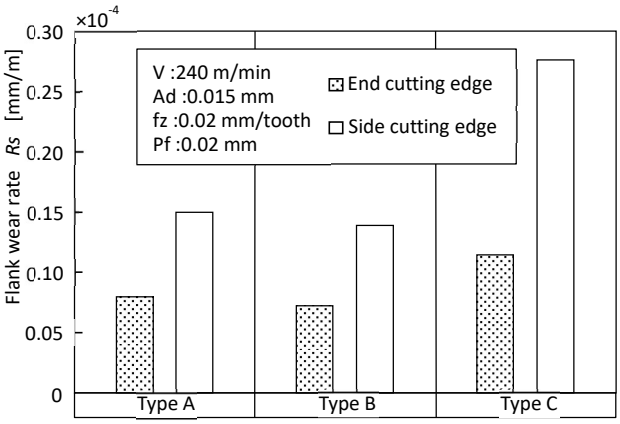

Figure 3. Comparison of flank wear rate for side and end cutting edge for three mist types

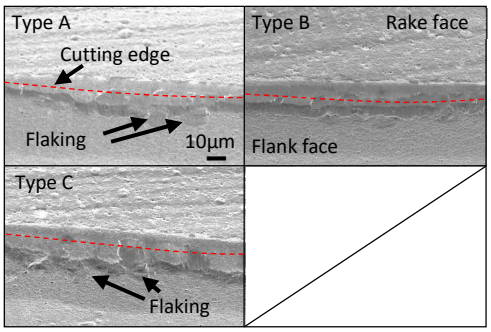

Figure 4. Comparison of flank wear in side cutting edge for three mist types

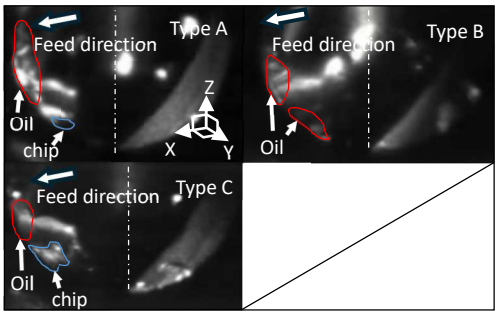

Figure 5. Comparison of side and end cutting edge supply conditions during cutting for three mist types

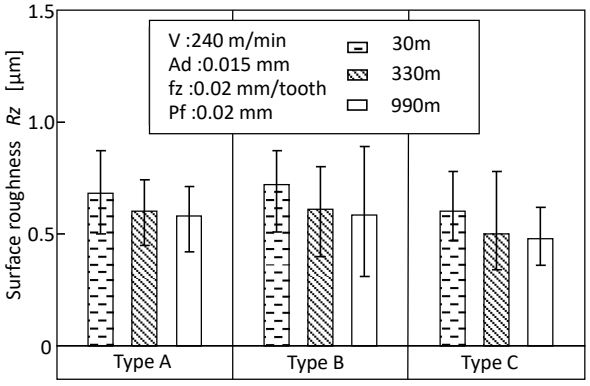

Figure 6. Comparison of surface roughness in cutting with increasing cutting length for three mist types

causing flaking of the coating. Type C had a hig-her flow velocity than that of Type A but a smaller spray angle and lower flow rate, preventing sufficient mist from being di-rectly supplied to the side cutting edges. This resulted in flaking and a higher wear

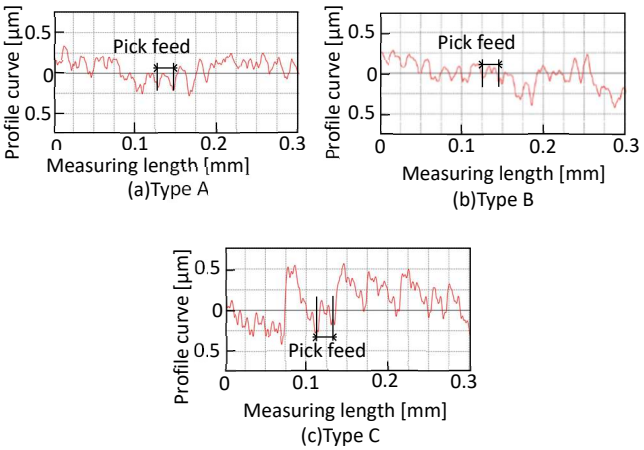

Figure 7. Comparison of profile curve at cutting distance of 990m for; (a)Type A, (b)Type B, and (c)Type C

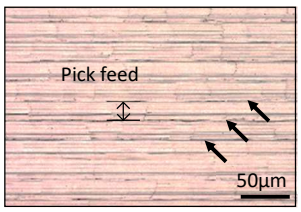

Figure 8. Machined surfaces for Type C and cutting distance of 990 m

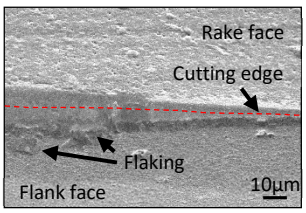

Figure 9. End cutting edge for Type C and cutting distance of 990 m

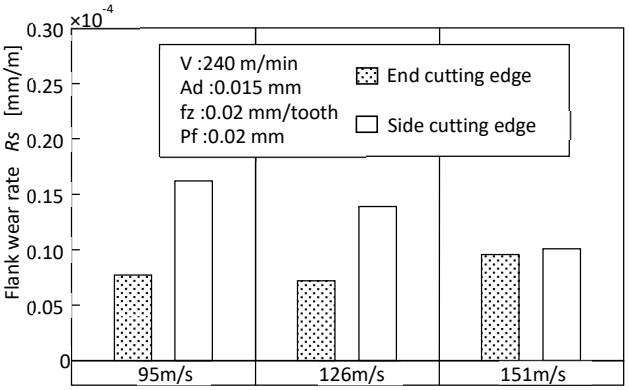

Figure 10. Comparison of flank wear rate for side and end cutting edge at various flow velocities for Type B

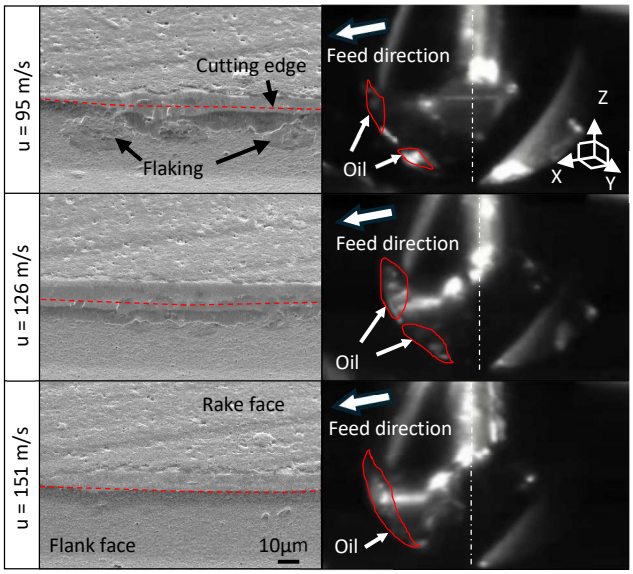

Figure 11. Comparison of flank wear in side cutting edge and the effect of side and end cutting edge supply conditions during cutting at various flow velocities for Type B

rate. For the end cutting edge, however, wear rates are similar across all mist types, as shown in Figure 3. As shown in Figure 5, lubricant was supplied to the end cutting edge flank for all mist types. For the end cutting edge, it can be inferred that there was no significant difference in the supply to the machining point, as all mist types entrained the lubricant adhering to the machined surface while rubbing the surface, resulting in only small differences. Figure 6 shows the variation in maximum height roughness (Rz) with increasing cutting distance for the three mist types. As indicated, the machined surface roughness Rz was approximately 0.5 μm for all mist conditions. As mentioned, the end cutting edge, which forms the machined surface, likely produced a similar surface roughness in all mist supply conditions because the supply to the machining point involved entraining the lubricant adhering to the machined surface while rubbing it. The profile curve was analysed for further surface evaluation. Figure 7 shows the profile curve for each mist type at a cutting distance of 990 m. Type A and Type B produced similar pick feeds, whereas Type C formed larger pick feeds. To analyse further, the machined surface was examined. Figure 8 shows the machined surface for Type C and cutting distance of 990 m. Type C, while showing a normal pick feed spacing, had larger convexities, which formed at the boundary between the end cutting edge and the side cutting edge. At this boundary, adhesion and tool damage caused by the flaking of agglomerated material may have led to excessive material removal and reduced cutting depth. Since Type C had a low flow rate, the amount of lubricant supplied to the machining point was limited, and as shown in Figure 9, the damage to the side cutting edge flank expanded towards the end cutting edge. Therefore, it can be inferred that a larger pick feed was formed for Type C.

3.2 Effect of mist flow velocity conditions on machining characteristics

Based on the above results, the effect of flow velocity on machining characteristics was investigated using Type B, which most effectively suppressed the progression of flank wear on the side cutting edge and allowed for adjustments to flow velocity. The flow velocity was set to 95 m/s, 126 m/s, or 151 m/s. Correspondingly, the flow rate was slightly adjusted to 3.37 ml/h, 3.59 ml/h, and 3.82 ml/h, respectively. The flow velocity of 126 m/s was the Type B velocity used in the previous section. Figure 10 shows the flank wear rates of the side and end cutting edges at each flow velocity. As shown, the wear rate of the side cutting edge decreases as the flow velocity increases. Figure 11 shows the wear condition of the side cutting edge at a cutting distance of 990m and the mist supply conditions captured by the high-speed camera. At flow velocities of 126 m/s and 151 m/s, wear progressed gradually. At a flow velocity of 95 m/s, adhesion and flaking were observed on the side cutting edge's flank surface. At a flow velocity of 151 m/s, sufficient oil was supplied to the side cutting edge's flank surface, indicating that the high flow velocity prevented mist disruption by the airflow generated by tool rotation. At a flow velocity of 126 m/s, oil reached the flank surface but did not fully cover the side cutting edge. Conversely, at a flow velocity of 95 m/s, the mist supply was insufficient, leading to machining. These results indicate that higher flow

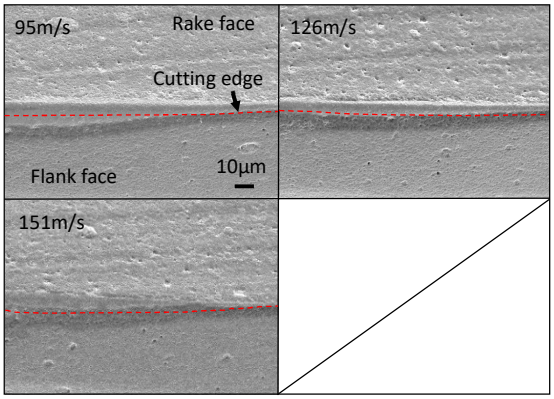

Figure 12. Comparison of flank wear in end cutting edge for three flow velocities

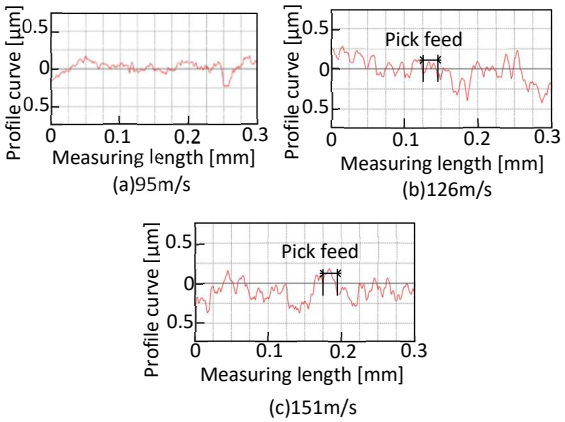

Figure 13. Comparison of profile curve at cutting distance of 990m for flow velocities of; (a)95m/s, (b)126m/s, and (c)151m/s

Figure 14. Machined surface obtained with flow velocity of 95 m/s at cutting distance of 990 m

velocities effectively reduce wear on the side cutting edge. Unlike the side cutting edge, the end cutting edge exhibited a similar wear rate across all flow velocities (Figure 10). Figure 13 shows the wear condition of the flank face of the cutting edge for the three flow velocities. As shown, wear progresses gradually for all mist conditions. The progressive wear observed in the end cutting edge at all flow velocities can be attributed to its smaller depth of cut compared to that of the side cutting edge. Furthermore, Figure 12 shows that oil was supplied to the end cutting edge at all flow velocities. This is likely due to the entrapment of oil adhering to the machined surface during cutting, rather than direct mist supply, which explains the lack of significant differences in wear. Additionally, since no significant differences were observed in the wear of the cutting edge forming the machined surface, the maximum height roughness (Rz) remained at approximately 0.5 μm regardless of the flow velocity. On the other hand, the cross-sectional profile showed different results at a flow velocity of 95 m/s. The cross-sectional curves for each flow velocity at a cutting distance of 990 m are shown in Figure 14. At flow velocities of 126 m/s and 151 m/s, pick feed clearly formed, whereas no pick feed formed at a flow velocity of 95 m/s. To analyse further, the machined surface was examined. Figure 15 shows the machined surface obtained with flow velocity of 95 m/s at cutting distance of 990 m. The surface had marks resembling those left by pressing, which are absent at higher flow velocities. The formation of the machined surface involves the side cutting edge abrading the material, followed by the end cutting edge abrading it during the subsequent pick feed. As shown in Figure 10, at a flow velocity of 95 m/s, the rapid progression of side cutting edge flank wear likely resulted in insufficient pick feed formation, causing a pressed-down machined surface. Based on the above, a higher flow velocity should be used to achieve stable surface roughness and pick feed in the formation of the machined surface.

4. Conclusions

In this study, the effect of mist spray conditions on machining characteristics was investigated by performing direct engraving milling on STAVAX using a small-diameter-ball end mill. It was found that a higher mist flow velocity enables the mist to be supplied directly to the machining point, thereby suppressing the progression of flank wear on the side cutting edge. On the other hand, the wear on the end cutting edge flank was not affected by the mist supply rate or mist flow velocity, as the oil adhering to the machined surface is entrained and supplied when the end cutting edge scrapes the surface. In addition, no changes were observed on the maximum height roughness (Rz) due to differences in mist supply or mist velocity. The pick feed was found to be affected by mist supply and mist velocity. When the mist flow rate was extremely low, the pick feed became large. When the mist flow velocity was low, the progression of wear on the flank surface of the side cutting edge accelerated and the pick feed did not properly form. These results suggest that a high mist velocity should be used to suppress wear on the side cutting edges and adhesion to the machined surface.

Acknowledgment

The authors gratefully acknowledge Fuji BC engineering for providing the experimental apparatus.

References

[1] S.N.B. Oiaei, Y. Karpat 2014 Experimental Investigations on Micro Milling of Stavax Stainless Steel *Procedia CIRP.* **14** 377-382
[2] Lee-Long Han, Chun-Ming Lin, Yih-Shiun Shih 2013 Corro sion Resistance of ASSAB Stavax ESR Stainless Steel by Heat and Cold Treatment *Materials Transactions.* **54** No.5 833-838
[3] L. Grandguillaume, S. Lavernhe, Y. Quinsat, C. Tournier 2015 Mold manufacturing optimization: a global approach of milling and Polishing processes *Procedia CIRP.* **31** 13-18
[4] P. Fallböhmer, C.A. Rodríguez, T. Özel, T. Altan 2000 High-speed machining of cast iron and alloy steels for die and mold manufacturing *Journal of Materials Processing Technology.* **98** 104-115
[5] K. Yamamoto, H. Wakamiya, Y. Hayakawa, Y. Iida, M. Takasaki, R. Kajitani, T. Sakaya, K. Hayashi 2019 A Study of Integrated Technogy Development for the Manufacture of Large Cemented Carbide Molds -Research on Tool Shape and Cutting Conditions for Highly Efficient Direct Cutting- *Quality Engineering*. **27** No. 5 321-329 (in Japanese)
[6] W.Y.H. Liew, Y.G. Lu, X. Ding, B.K.A. Ngoi, S. Yuan 2004 Performance of uncoated and coated carbide tools in the ultra-precision machining of stainless steel *Tribology Letters.* **17** 851-857
[7] T.Thepsonthi, M.Hamdi, K.Mitsui 2009 Investigation into minimal-cutting-fluid application in high-speed milling of hardened steel using carbide mills *International Journal of Machine Tools & Manufacture.* **49** 156-162